Response of the MDT filled with $Ar+5\%CO_2+3\%CH_4$ to thermal neutrons

S.Borzakov, I.Boyko, G.Chelkov, V.Dodonov, M.Ignatenko, M.Nikolenko, A.Nozdrin, I.Pisarev

JINR, Dubna, Russia

Abstract

The sensitivity of aluminum drift tubes to thermal neutrons has been measured using the neutron beam of the JINR IBR-2 pulsed reactor. The tube tested was filled with an Ar + 5%CO_2 + 3%CH_4 gas mixture at pressures from 1 to 4 atm. For the tested tube with 0.4 mm wall thickness the measured efficiency was $(6.3\pm0.4)\times10^{-4}$ at a gas pressure of 3 atm. The tube sensitivity is dominated by absorption of the neutrons in the tube wall followed by beta decay of ^{28}Al and ^{56}Mn nuclei. The efficiency also depends on the gas pressure (from (5.6 ± 0.6)% of the total efficiency at 1 atm to (19 ± 2)% at 4 atm) mainly due to activation of argon in the process of neutron absorption by ^{40}Ar nuclei. The average energy deposition of the thermal neutrons is approximately the same as for minimum ionizing particles and is equal to 20 keV at a gas pressure of 3 atm.

Introduction

According to the results of Monte Carlo simulation on the occupancy in the detector elements of the ATLAS [1] muon system (monitored drift tubes), the most dangerous background is due to low energy photons and neutrons [2]. If the spectrum of neutrons is assumed to decrease with energy as 1/E, a large contribution to the neutron background is given by thermal neutrons. From the drift tube (DT) aging point of view, it is vital to know the sensitivity of the DT to thermal neutrons and the average neutron energy deposition in order to choose an appropriate gas and working point.

In our previous measurements [3] of DT sensitivity to neutrons of different energies an upper limit on the DT efficiency to intermediate energy neutrons was established at a level of 10^{-3} and the sensitivity to fast neutrons was measured. Unfortunately, it was impossible to measure the tube efficiency to neutrons with energies lower than 5 eV. Though the efficiency of different types of muon detectors to neutrons has already been measured with radioactive neutron sources[4, 5] and a neutron beam[6], there is only one experimental work[4], where the efficiency of an aluminum drift tube, a mylar tube and a cathode strip chamber to thermal neutrons was measured. Using a ^{252}Cf source, a 9 cm polyethylene moderator and a 1 mm cadmium absorber the authors obtained an efficiency at the level of $(1.2\text{-}3)\times10^{-3}$. However the measured efficiencies were essentially dependent on the gas type used, and it seemed strange that the mylar tube with the same construction parameters had shown larger efficiency than the aluminum tube. Contribution of radioactivation of the muon detector material to the total efficiency was estimated at a level of only 50%. The origin of another 50% of efficiency was not identified. The tube response to thermal neutrons was slightly higher than to minimum ionizing particles.

It should be noted that while fast neutrons are mainly detected in DT via recoil nuclei[3, 4], thermal neutrons can only be detected due to their absorption in the tube wall or in the gas mixture followed by a radioactive decay.

Experimental procedure

One of the main problems in measuring of the DT efficiency to neutrons is a large gamma background from a neutron source. The gammas are produced in radioactive decays of different nuclei that are the products of nuclear capture in a neutron source or in a nuclear reactor. Since the DT sensitivity to gammas [8] is at least 10 times higher than the sensitivity to neutrons, special measures should be taken. Our measurements have been performed using the thermal neutron channel of the JINR IBR-2 pulsed reactor [9]. This reactor has an average thermal power of 2 MW, a peak power of 1500 MW, and the power released between pulses is about 0.1 MW. The repetition rate of neutron pulses is 5 Hz and the half-width of the fast neutron pulse is 215 μs. The scheme of the neutron channel is shown in Fig. 1. The beam of thermal neutrons was formed by a system of collimators located just behind the reactor moderator. Then the neutrons went along a bent 24-m long neutron guide pipe. The guide pipe consisted of 24 empty rectangular glass sections, 1 m long each. The cross section of the neutron guide was 140×15 mm^2. The glass walls were polished inside and plated by nickel to reflect the thermal neutrons falling on the glass surface at angles smaller than 4^o. The guide sections were connected with each other in such a manner that the neutron guide had a bending radius of 2000 m. Along the neutron guide, there were two catchers for absorption of fast neutrons and direct gammas from the reactor. The bending neutron guide let pass the neutrons with energy lower than 0.1 eV and suppressed the fast neutron background by a factor of 10^5.

Two beam intensity monitors were used [9]. The first one was located 2 m downstream from the tested tube and consisted of 12 He^3-filled proportional counters which surrounded a lead target 80 mm in diameter and 5 mm thick. The thermal neutrons were scattered in the lead target and then were detected in the proportional counters. The second monitor was a usual fission chamber with a small amount of ^{235}U inside. The calibration of both monitors and the absolute neutron flux measurements were made by the activation method using a 200 μm thick copper foil. A typical neutron flux at the tube location was $5.7{\cdot}10^5$ cm^{-2}s^{-1} that corresponds to $2.6\cdot10^6$ s^{-1} in the irradiated tube section. Neutrons in the beam had energies in the range 0.001eV-0.2eV.

The DT tested was an aluminum tube 20 cm in length, 3 cm in diameter and with wall thickness 0.4 mm. The anode of the DT was a tungsten wire 50μm in diameter. The tube was located at the end of the beam guide (see Fig. 1). Only 15 mm of the tube length were irradiated. The gas mixture was Ar + 5%CO_2 + 3%CH_4. High voltages were set so that the gas gain was about 7×10^4. Tube signals were amplified and fed to a discriminator. The threshold of the discriminator was measured with ^{55}Fe and corresponded to 13 electrons of primary ionization at a gas pressure of 1 atm. The pulse heights of the tube signals were measured by a charge digital converter ADC (LeCroy 2249W). For the time measurements, the internal clock of a PC was used. It was synchronized with a reactor burst. A two-dimensional time-amplitude histogram was filled during the measurements. Time spectra, obtained by projecting the time-amplitude histogram, were then corrected for nonzero ADC readout and conversion time (150 μs). Pure time spectra were also measured reading the fast scaler every 100 μs. This method allowed the time spectrum to be measured at count rates up to few MHz without significant loss of counts.

Results

Fig. 2 shows the time dependence of the count rates of the monitor and the tube tested together with the background time spectrum. The background measurements were performed when the tube was removed from the beam and placed near the end of the neutron guide. In the spectra, one can see sharp peaks that correspond to a moment when the fast neutrons and gammas that were not absorbed in the catchers reached the DT. About 10 ms later, peaks that correspond to the thermal neutrons are clearly seen. There are also small peaks in the time spectra of both the DT and the monitor. They are separated by a fixed time interval and arise due to features of the reactor design. The main difference between the monitor and tube spectra is a high constant background in the time spectrum of the DT. Besides, there is slight difference in the form of the peaks in the region of thermal neutrons. After background subtraction, $(86.4\pm0.3)\%$ of total counts of the tube filled with a gas mixture at 1 atm are at constant count rate, $(6.0\pm0.5)\%$ are due to fast neutrons and gammas from the reactor burst and only $(7.6\pm0.5)\%$ of counts correspond to the moment when the main part of the thermal neutrons pass through the DT.

The source of the large constant count rate is neutron activation of different elements of the tube material. The main contribution to this process is the production of ^{28}Al in the reaction of neutron absorption by ^{27}Al followed by beta decay of the ^{28}Al nucleus (half-life is 2.3 min[10]). This is confirmed by the time dependence of the count rate after the beginning of the tube irradiation (Fig. 3) and the decay curve of the induced activity after beam shutdown (Fig. 4). The curves in this figures are fits of the data by activation and decay type expressions. The resulting half-lives obtained from the fit were 2.23 ± 0.02 and 2.34 ± 0.10 min, which is consistent within the errors with the half-life of ^{28}Al. An additional mechanism is activation of manganese nuclei. Though the quantity of manganese is not more than 0.5% in the aluminum alloy of the DT wall, the cross section of production of ^{56}Mn (half-life 155 min) is 57 times larger than the cross section of Al activation. Since the half-life of ^{56}Mn is much larger than that of aluminum, this element practically doesn't change the time constant in the fit of the activation or decay curves. It only affects the value of the constant term.

Fig. 5 shows the dependence of the constant count rate on the tube wall thickness. The change in the tube wall thickness was made by wrapping the tube in additional aluminum sheets. The efficiency of the tube significantly depends on the wall thickness. The extrapolation of the experimental data to zero wall thickness has shown that not only wall materials were activated. The additional mechanism affecting the DT efficiency is the production of ^{41}Ar in the process of neutron absorption by the ^{40}Ar nucleus of natural argon. The ^{41}Ar nucleus then β-decays with half-life of 109 min[10]. This mechanism should manifest itself in the dependence of the tube count rate on the gas pressure. The experimental results corresponding to the discriminator level of 25 primary electrons are shown in Fig. 6. Extrapolation to zero gas pressure gave a contribution of the tube wall activation to the total tube efficiency. At 1 atm gas pressure, the wall activation accounts for $(94.3\pm0.5)\%$ of the full efficiency. The contribution of argon activation to the total efficiency varies from (5.6±0.6)% at a gas pressure of 1 atm to (19±2)% at 4 atm.

The origin of the peak in the time spectrum which corresponds to the time interval when the main part of the thermal neutrons pass through the tube is believed to be from gamma background. This background was produced in the interactions of the thermal neutrons with the environment, mainly with air and different construction components of the neutron channel. Fig. 7 shows the change of the constant level and the thermal peak contributions to the count rate with the thickness of the lead absorber between the tube and the exit from the neutron guide. The attenuation of the constant level behaves according to the absorption of the thermal neutrons in lead, but the thermal peak increases at first and only for lead thickness more than 4 cm it slowly decreases. This means that the peak is due to production of gammas in the lead absorber by thermal neutrons. The study of the background in different places of the experimental hall and with different absorbers in the beam path also showed that the magnitude of this peak significantly depended on the presence of materials in the path of the beam.

Thus, one can obtain the DT efficiency dividing the constant count rate by the neutron flux through the tube. The result was $(6.3\pm0.4)\times10^{-4}$ at 3 atm gas pressure.

Based on cross sections of radiative absorption of thermal neutrons by aluminum, manganese and argon nuclei, one can estimate the efficiency of the aluminum tube to thermal neutrons. With 0.231 b for the cross section of thermal neutron absorption by Al, 13.3 b for Mn and 0.66 b for Ar nuclei [10], the total probabilities of the production of ^{28}Al, ^{56}Mn and ^{41}Ar nuclei are $1.66\cdot10^{-3}$, $0.24\cdot10^{-3}$ and $0.42\cdot10^{-4}$ respectively. Since not all the electrons produced in the tube wall reach the sensitive volume of the DT, one should introduce detection probability of Al and Mn decays. We have evaluated this factor using the tables of electron ranges in aluminum[11] and taking into account the geometrical parameters of the tube. For energy distribution of electrons from beta decay the spectrum for allowed decays of ^{28}Al and ^{56}Mn was used[12]. Calculations gave 0.39 for ^{28}Al and 0.33 for ^{56}Mn. The tube efficiency at 1 atm gas pressure is then combined of $6.3\cdot10^{-4}$ from Al, $0.8\cdot10^{-4}$ from Mn and $0.42\cdot10^{-4}$ from Ar activation, which is in good agreement with experimental data.

Another question is the influence of adjacent tubes on the count rate. A muon chamber consists of several layers of tubes glued together. When the chamber is irradiated by neutrons, the count rate of one specific tube is combined from the count rate induced by particles originated in the tube itself and the count rate induced by particles originated in the surrounding tubes. To study this question, we placed various configuration of tubes (see Fig. 8) in the beam and measured the count rate of one operational tube (shown on the figure with the anode wire). The measured ratio of count rates between cases 2 and 1 is 1.7 and ratio of count rates between the cases 3 and 1 is 2.0. So we should expect the count rate of DT assembled in the chamber to increase two times compared to the single tube count rate. It is apparently so because high energetic electrons produced in ^{28}Al decay can pass through the DT wall. Besides of that, the presence of any material in the vicinity of DT can also increase the tube count rate induced by thermal neutrons.

Simultaneously with the DT efficiency measurements, the pulse height spectra of the tube signals were also studied. Fig. 9 shows a typical pulse height spectrum. Percentage of streamer signals was negligible (< 0.2 %). The dependence of an average amplitude on time is shown in Fig. 10. There was some degradation of the signal amplitudes at the moment when fast neutrons and gammas from the reactor burst reached the tube. This effect was mainly due to an electronics overshoot and to a space charge effect, which was caused by a large count rate at that moment (about 60 kHz). The average energy deposition corresponding to the pulse of a thermal neutrons is approximately the same as for minimal ionizing particles and equals to 20 keV at 3 atm.

Conclusions

With a special beam of thermal neutrons from the JINR pulsed reactor IBR-2, the DT response to thermal neutrons have been measured. The results show that the tube efficiency is mainly defined by activation of aluminum and manganese in the tube wall and argon in the gas mixture. Its value is $(6.3\pm0.4)\times10^{-4}$ at a gas pressure of 3 atm. Since the spectra of electrons in beta-decay of ^{28}Al and ^{56}Mn are sufficiently hard (the maximum energy in ^{28}Al decay is about 2.8 MeV), the efficiency strongly depends on the wall thickness. Activation of aluminum and manganese for a tube with 0.4 mm wall thickness gives $(5.4\pm0.3)\times10^{-4}$. The contribution to the total efficiency from argon activation changes from (5.6 ± 0.6)% at 1 atm gas pressure to (19 ± 2)% at 4 atm. Good agreement between the measured and the calculated efficiency is observed. We did not see any additional appreciable mechanisms contributing to the DT efficiency to thermal neutrons.

The average deposited energy of the single pulse in the process of thermal neutron detection by an aluminum tube is approximately the same as for minimum ionizing particles (20keV).

We would like to thank V.I.Luschikov, V.V.Golikov and V.L.Malyshev for the useful discussions and help at the first stage of this work.

References

[1] ATLAS, Technical Proposal for a General-Purpose pp Experiment at the Large Hadron Collider at CERN, CERN/LHCC/94-43, LHCC/P2, 15 December 1994.

[2] G.Battistoni, A.Ferrari and P.R.Sala, Muon Chamber sensitivity of neutron and photon background in the ATLAS hall. ATLAS Internal Note MUON-NO-052, 1994.

[3] G.A.Chelkov et al., Investigation of spectral efficiency of pressurized drift tubes for detection of neutrons in the energy range 5 eV and 200keV. ATLAS Internal Note MUON-NO-031, 1993.

[4] S.Boyarinov et al., Neutron and Gamma sensitivity of gas detectors. GEM NOTE TN-93-345, SSC LAB (1993).

[5] A.Korytov et al., Nucl. Instr. & Meth. in Phys. Res. A 338 (1994) 375.

[6] A.S.Denisov et al., Differential sensitivity of cathode strip chambers to neutrons and photons. ATLAS Internal Note MUON-NO-033, 1994. Preprint PNPI No. 1941 Dec.1993.

[7] M.Angelone et al., Nucl. Instr. & Meth. in Phys. Res. A 355 (1995) 399.

[8] S.Baranov et al., Gamma Sensitivity of Pressurized Drift Tubes. ATLAS Internal Note MUON-NO-036, 1994.

[9] E.Dermendjiev et al., An experimental facility for studying delayed neutron emission. JINR preprint E13-93-6, 1993.

[10] T.S.Belanova et al., Radiation neutron absorption. Handbook. Energoatomizdat. Moscow. 1989. (In Russian).

[11] M.Berger, S.Seltzer. Tables of Energy Losses and Ranges of electrons and positrons. NASA SP-3012, 1964.

[12] B.S.Dzhelepov, L.N.Zyrjanova and Yu.P.Suslov. Beta-Processes. Functions for beta-spectra and electron capture analysis. Nauka. Leningrad, 1972. (In Russian).

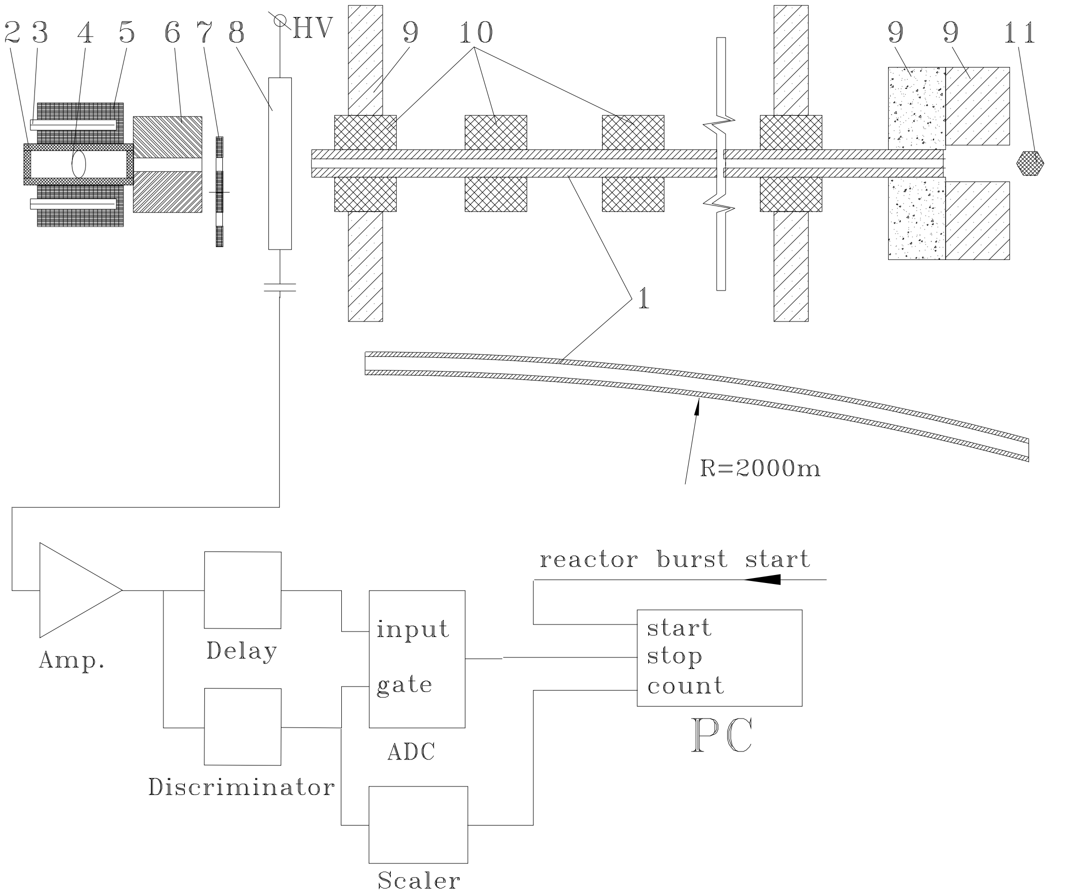

Figure 1: Schematic view of the neutron channel, experimental arrangement layout and electronics used. 1 – mirror neutron guide, 2 – Cd cylinder, 3 – neutron counters, 4 – target, 5 – moderator, 6 – collimator, 7 – chopper, 8 – drift tube, 9 – shielding, 10 – catchers, 11 – reactor core.

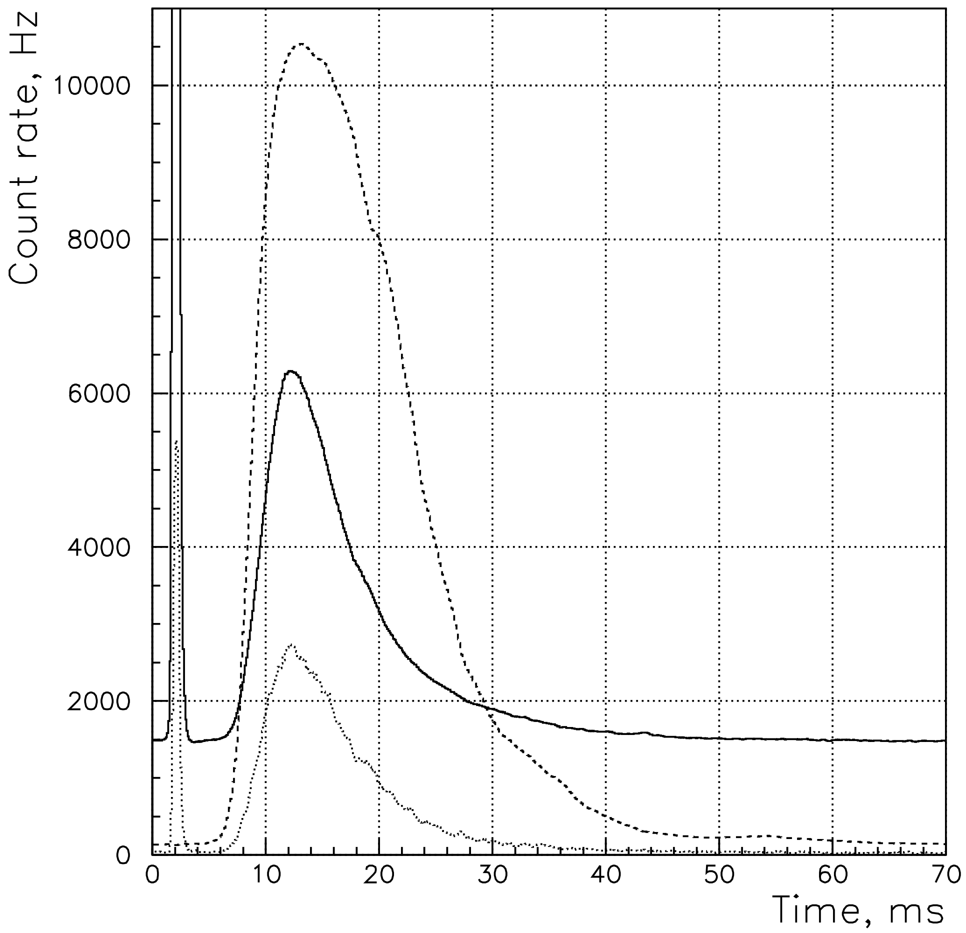

Figure 2: The time spectra measured by monitor (dashed curve) and DT (solid line). Dotted curve represents background, measured by DT placed out of the beam.

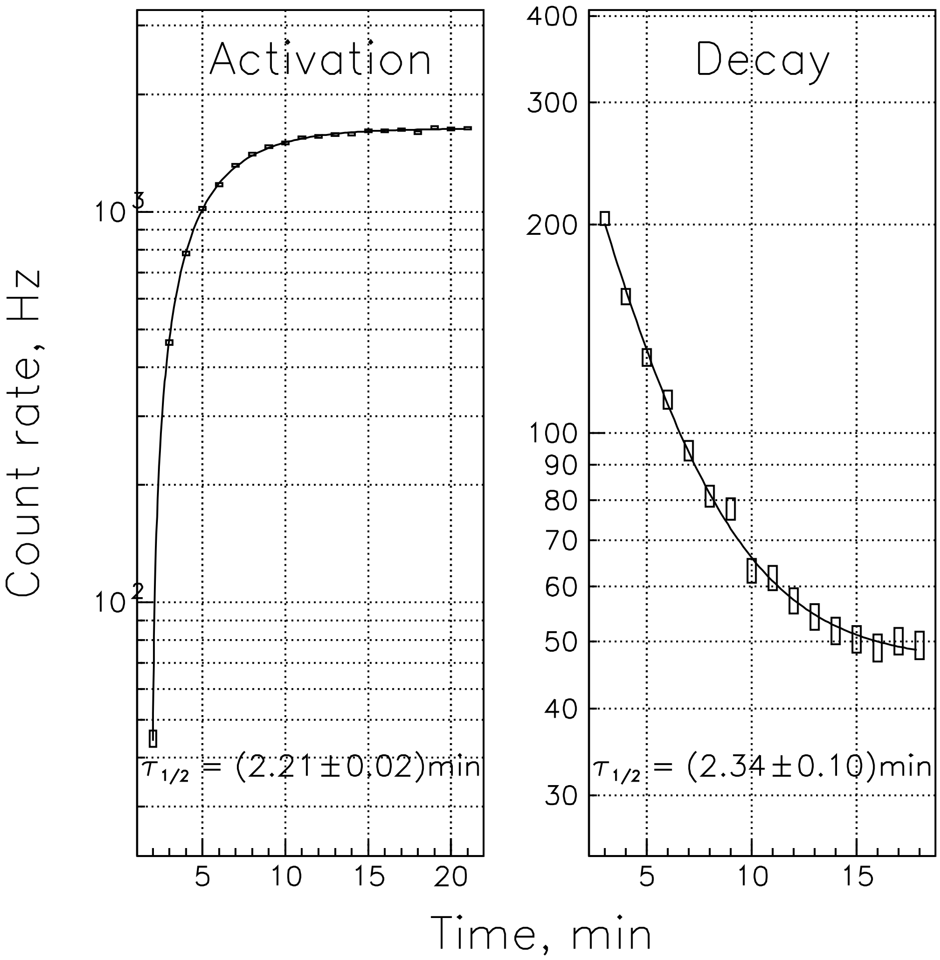

Figure 3: The tube count rate versus time after beginning of irradiation.

Figure 4: The tube count rate versus time after few hours of irradiation.

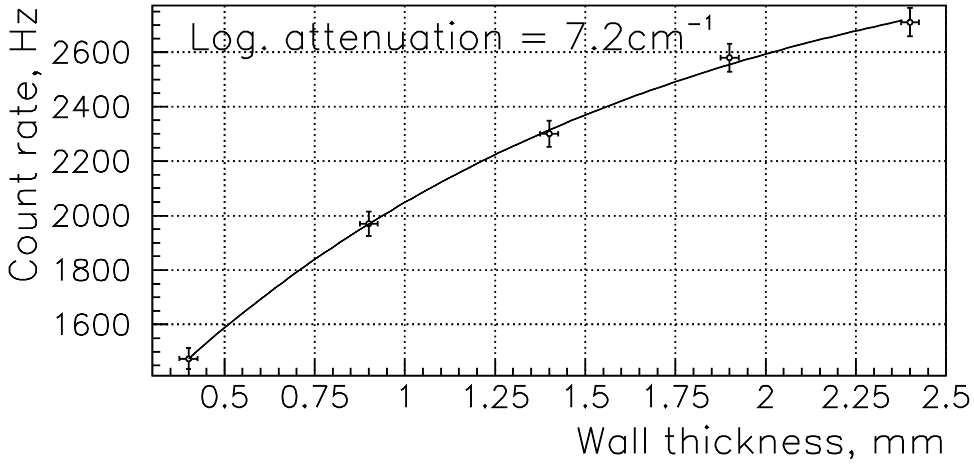

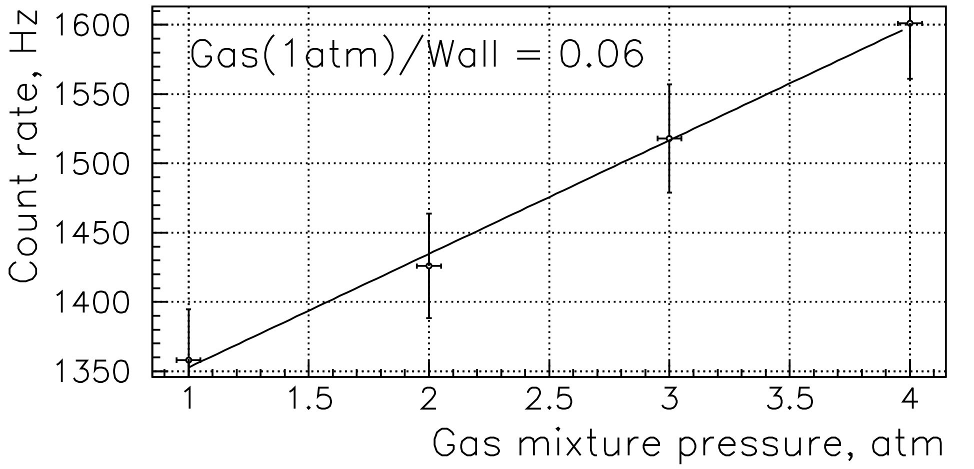

Figure 5: The tube count rate versus thickness of the aluminum wall.

Figure 6: The tube count rate versus gas mixture pressure.

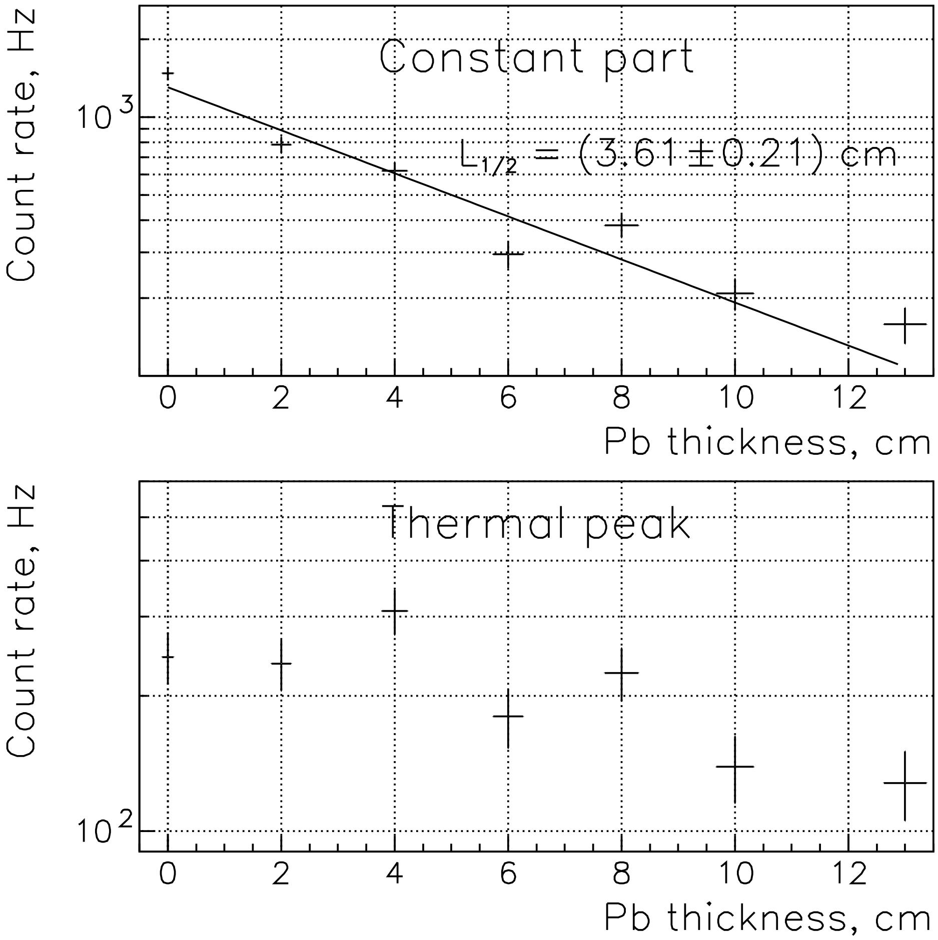

Figure 7: Dependence of the spectrum constant level and of the thermal peak on thickness of the lead absorber.

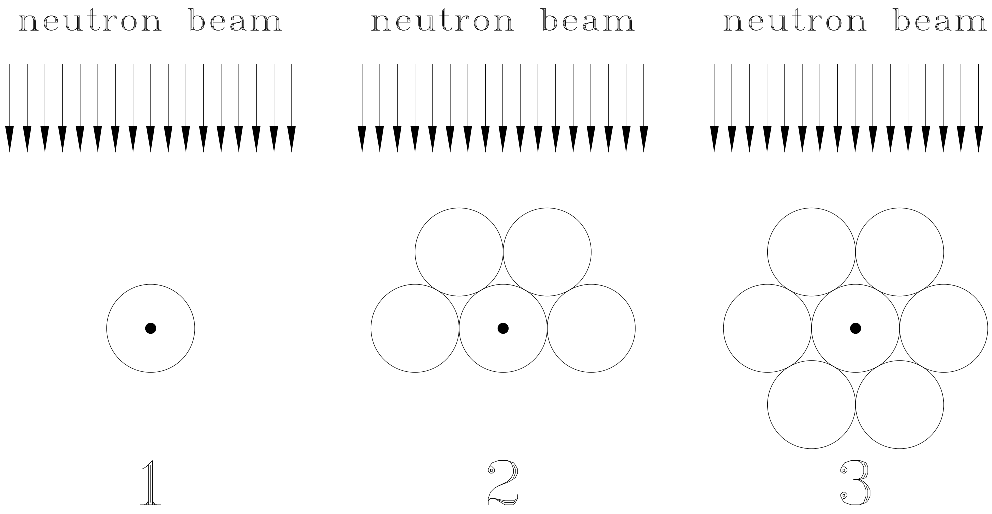

Figure 8: Setup for determining of the influence of surrounding tubes.

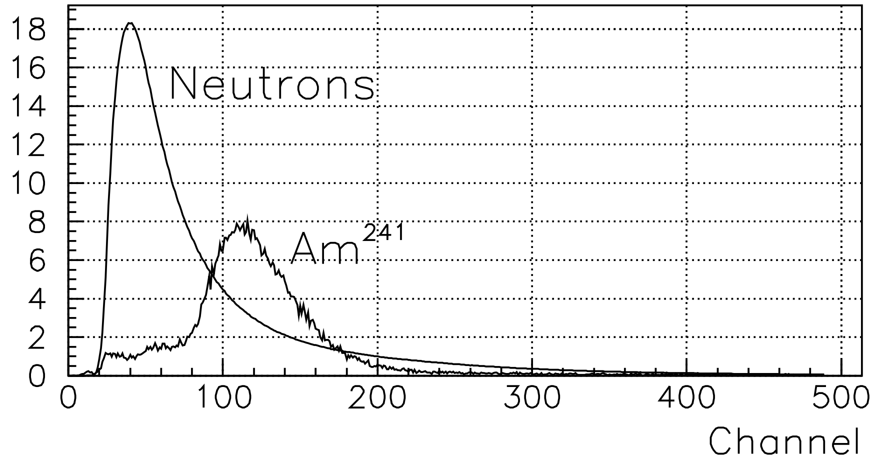

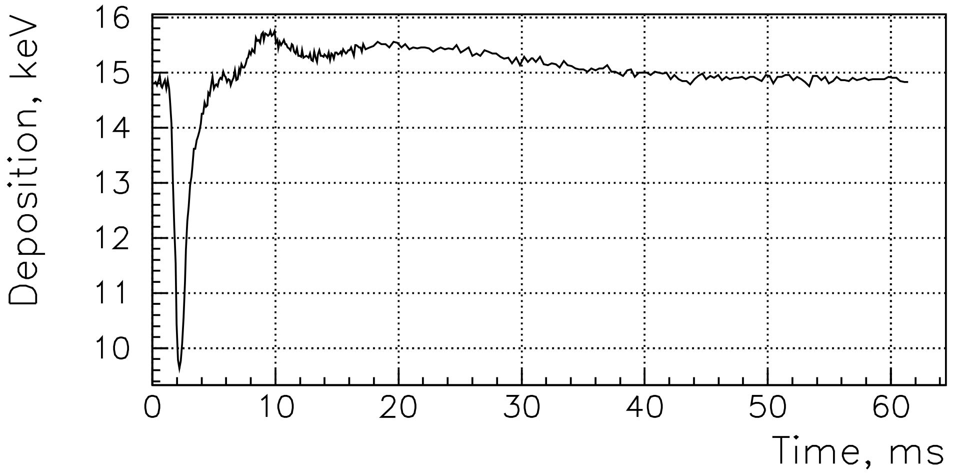

Figure 9: Typical amplitude spectrum of the tube signals for thermal neutrons and for ^{241}Am source.

Figure 10: Time dependence of the average energy deposition in the tube.